

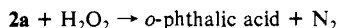
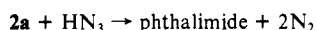
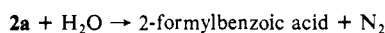
# Nucleophilic Addition to Diazaquinones. Formation and Breakdown of Tetrahedral Intermediates in Relation to Luminol Chemiluminescence

Gábor Merényi,\* Johan Lind, and Trygve E. Eriksen

Contribution from the Departments of Physical and Nuclear Chemistry, The Royal Institute of Technology, S-100 44 Stockholm, Sweden. Received April 28, 1986.

Revised Manuscript Received July 19, 1986

**Abstract:** Nucleophilic addition to diazaquinones **2** was shown to occur at the carbonyl group. The rate constants and activation parameters for this process were determined with a large number of nucleophiles. The kinetics was rationalized in terms of an equilibrium reaction between the reactants and a tetrahedral intermediate followed by the latter's breakdown. With some nucleophiles the enthalpy of activation for this process was found to be essentially zero. These cases were interpreted by assuming the formation of the tetrahedral intermediate to be the rate-determining step in the consumption of the diazaquinone. The complete mechanisms of hydrolysis, azidolysis, and perhydrolysis were investigated. The stoichiometries were found to be



The breakdown kinetics of the tetrahedral intermediate of **2** with  $\text{H}_2\text{O}_2$  was determined by chemiluminescence measurements while the lifetimes of the corresponding adducts of  $\text{OH}^-$  and  $\text{N}_3^-$  were estimated from experiment. The initial additions of  $\text{OH}^-$  and  $\text{N}_3^-$  were shown to generate acyldiazene species. The latter were prone to further nucleophilic addition of  $\text{OH}^-$  or  $\text{N}_3^-$  to the acyldiazene group. This second addition is also proposed to proceed via a tetrahedral intermediate the breakdown of which is exothermic involving the expulsion of  $\text{N}_2$ . In the hydrolysis this step yields the end product (2-formyl benzoate) while in the azidolysis a second expulsion of  $\text{N}_2$  occurs which is followed by ring closure and tautomerization to yield the phthalimide. The neutral breakdown of the  $\text{H}_2\text{O}_2$  adduct of **2** yields ground-state phthalate while its  $\text{OH}^-$ -catalyzed rupture leads to chemiexcitation. The latter process is proposed to involve as an intermediate an acyldiazene peracid anion. This species is prone to intramolecular nucleophilic addition to yield a cyclic tetrahedral intermediate. The breakdown of the latter through the expulsion of  $\text{N}_2$  generates an antiaromatic endoperoxide which transforms into excited phthalate in a pericyclic process.

In the past decades our knowledge of the chemistry of carbonyl compounds such as aldehydes, ketones, and esters has reached a remarkably high degree of sophistication.<sup>1-4</sup> This holds particularly true of nucleophilic additions to these compounds. Thus, both final products and intermediates have been identified, and overall mechanisms have been elucidated in detail.

In contrast, the study of nucleophilic addition to quinones has disclosed few kinetic details. Indeed, most investigations have been restricted to the identification and quantification of the end products.<sup>5</sup> The latter are invariably substituted at a carbon-carbon double bond of the quinone. Therefore, the prevailing view is that the initial nucleophilic attack occurs equally at a  $\text{C}=\text{C}$  bond of the quinone.

Diazaquinones constitute a rather interesting class of quinones. Qualitatively, they exhibit redox properties similar to those of quinones. Thus, one can observe the various reactions involving semiquinones and hydroquinones (cyclic hydrazides). Quantitatively, however, the reduction potentials of diazaquinones are more positive by about 300 mV than those of the isoelectronic quinone analogues.<sup>6</sup> Since positive redox potentials usually are connected with high reactivities toward nucleophiles, the electrophilicities of diazaquinones are expected to exceed by several orders of magnitude those of typical quinones. Indeed, with some diazaquinones, the rate constants for the addition of  $\text{OH}^-$  and  $\text{HO}_2^-$  were found to approach the diffusion controlled limit.<sup>7</sup>

## Scheme I

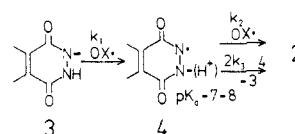


Table I. Second-Order Rate Constants of Pertinent Radical Reactions

reaction	$k$ or $2k$ ( $\text{mol}^{-1} \text{dm}^3 \text{s}^{-1}$ )	ref
$3(\mathbf{a-f}) + \text{N}_3^{\bullet} \rightarrow 4(\mathbf{a-f}) + \text{N}_3^-$	$k_1 \geq 2 \times 10^9$	this work
$3(\mathbf{a-f}) + \text{CO}_3^{\bullet-} \rightarrow 4(\mathbf{a-f}) + \text{CO}_3^{2-}$	$k_1 \geq 8 \times 10^8$	this work
$4(\mathbf{a-f}) + \text{N}_3^{\bullet} \rightarrow 2(\mathbf{a-f}) + \text{N}_3^-$	$k_2 \geq 10^9$	this work
$4(\mathbf{a-f}) + \text{CO}_3^{\bullet-} \rightarrow 2(\mathbf{a-f}) + \text{CO}_3^{2-}$	$k_2 \geq 10^9$	this work
$4(\mathbf{a-f}) + 4(\mathbf{a-f}) \rightarrow 2(\mathbf{a-f}) + 3(\mathbf{a-f})$	$5 \times 10^8 \leq 2k_3 \leq 2 \times 10^9$	this work
$\text{OH}^{\bullet} + \text{N}_3^- \rightarrow \text{OH}^- + \text{N}_3^{\bullet}$	$1.1 \times 10^{10}$	14
$\text{OH}^{\bullet} + \text{CO}_3^{2-} \rightarrow \text{OH}^- + \text{CO}_3^{\bullet-}$	$3.65 \times 10^8$	15

Given sufficiently rapid detection techniques such high initial reactivities may facilitate mechanistic investigations since the intermediates are formed so rapidly that they can be observed and kinetically studied.

There are many observations to show that initial nucleophilic attacks occur at the carbonyl groups of diazaquinones and that these attacks may engender tetrahedral intermediates: (a) the end products of hydrolysis contain aldehyde acids and molecular nitrogen;<sup>8,9</sup> (b) more than 1 equiv of  $\text{N}_2$  is released upon the

(1) Jencks, W. P. *Catalysis in Chemistry and Enzymology*; McGraw-Hill: New York, 1968.

(2) Jencks, W. P. *Acc. Chem. Res.* **1976**, *9*, 425.

(3) Funderburk, L. H.; Aldwin, L.; Jencks, W. P. *J. Am. Chem. Soc.* **1978**, *100*, 5444.

(4) Capon, B.; Dosunmu, M. I.; de Sanches, M. *Adv. Phys. Org. Chem.*; Gold, V., Bethell, D., Eds.; Academic Press: London, 1985; Vol. 21, pp 37-98.

(5) Finley, V. T.; *The Chemistry of Quinonoid Compounds, Part 2*; Patai, S., Ed.; John Wiley: London, 1974; pp 877-1144.

(6) Merényi, G.; Lind, J.; Eriksen, T. E. *J. Phys. Chem.* **1984**, *88*, 2320.

(7) Eriksen, T. E.; Lind, J.; Merényi, G. *J. Chem. Soc., Faraday Trans. 1* **1983**, *79*, 1493.

(8) Rusin, B. A.; Leksin, A. N. *Izv. Akad. Nauk SSSR Ser. Khim.* **1982**, *12*, 2685.

**Table II.** Measured Second-Order Rate Constants of Nucleophilic Attack on Diazaquinones at 25 °C (mol<sup>-1</sup> dm<sup>3</sup> s<sup>-1</sup>)

nucleophile	diazquinone			
	2a	2f	2b	2c
H <sub>2</sub> O <sup>a</sup>	4.0	1.3	0.45	1.7
OH <sup>-</sup>	5 × 10 <sup>7</sup>	2.0 × 10 <sup>7</sup>	4.0 × 10 <sup>6</sup>	1.1 × 10 <sup>7</sup>
H <sub>2</sub> O <sub>2</sub>		1.2 × 10 <sup>2</sup>	1.1 × 10 <sup>2</sup>	1.3 × 10 <sup>2</sup>
HO <sub>2</sub> <sup>-</sup>	3 × 10 <sup>8</sup>	2.0 × 10 <sup>8</sup>	5.0 × 10 <sup>7</sup>	1.1 × 10 <sup>8</sup>
H <sub>2</sub> S		1.3 × 10 <sup>4</sup>		
HS <sup>-</sup>		2.1 × 10 <sup>8</sup>		
I <sup>-</sup>			2.0 × 10 <sup>2</sup>	
Br <sup>-</sup>		<0.3	<0.1	<0.4
HCN		<0.3	<0.1	<0.4
CN <sup>-</sup>		2.0 × 10 <sup>5</sup>		4.0 × 10 <sup>4</sup>
HN <sub>3</sub>	2 × 10 <sup>5</sup>	1.3 × 10 <sup>5</sup>		
N <sub>3</sub> <sup>-</sup>	2.8 × 10 <sup>3</sup>	1.6 × 10 <sup>3</sup>	2.6 × 10 <sup>2</sup>	3.8 × 10 <sup>2</sup>
HSCN		>5 × 10 <sup>5</sup>		
SCN <sup>-</sup>		7.8 × 10 <sup>3</sup>	6.7 × 10 <sup>2</sup>	1.2 × 10 <sup>3</sup>
aniline		4.3 × 10 <sup>5</sup>	2.4 × 10 <sup>4</sup>	
NH <sub>3</sub>			(7 ± 2) × 10 <sup>2</sup>	
C <sub>2</sub> H <sub>5</sub> NH <sub>2</sub>			(3 ± 0.5) × 10 <sup>5</sup>	

<sup>a</sup>The values are pseudo-first-order rate constants (s<sup>-1</sup>).

reaction of N<sub>3</sub><sup>-</sup> with some diazaquinones;<sup>7</sup> (c) cyclic hydrazides (hydrodiazquinones) substituted at the ring nitrogens are stable compounds which do not release N<sub>2</sub>.<sup>10</sup> The present work is an effort to place nucleophilic addition to diazaquinones on a more quantitative footing.

More specifically, the entire mechanism of hydrolysis, azidolysis, and perhydrolysis will be investigated from the initial step through the formation of the end products. Chemiluminescence, which results from the perhydrolysis of certain diazaquinones, will be especially focussed upon with the aim of placing it into the general context of nucleophilic addition.

### Experimental Section

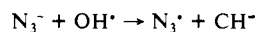
**Stopped Flow Measurements.** Diazaquinones can be produced by the oxidation of the corresponding hydrazide by ClO<sub>2</sub><sup>9</sup> according to Scheme I. By mixing aqueous solutions of ClO<sub>2</sub> and a particular hydrazide at neutral pH in a High-Tech stopped flow equipment with sequential mixing option, the time required for an 85% conversion of the hydrazide into the diazaquinone was determined. In addition the stability of the latter with respect to hydrolysis at pH 7 was obtained. With a fivefold excess of hydrazide over ClO<sub>2</sub> the consumption of ClO<sub>2</sub> observed at 360 nm as well as the formation of the diazaquinone followed first-order kinetics. At pH 7 the second-order rate constants *k* obtained from the above measurements were 1.5 × 10<sup>5</sup>, 3 × 10<sup>5</sup>, 10<sup>6</sup>, and 1.5 × 10<sup>6</sup> M<sup>-1</sup> s<sup>-1</sup> for the hydrazides 3a, 3f, 3b, and 3c.

The hydrolysis rates of the diazaquinones studied were always <4 s<sup>-1</sup> (see Table II). To study the nucleophilic addition to the diazaquinone the stopped flow apparatus was used in sequential mode where the diazaquinone was produced according to Scheme I in a premixing chamber.

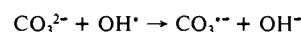
After a delay of 50 ms final mixing was achieved in the analysis chamber by mixing equal volumes of the mildly buffered neutral premixed solution with another solution buffered at the appropriate pH and containing the nucleophile under study. Hydrazide concentrations between 10<sup>-4</sup> to 10<sup>-3</sup> were employed with the lower value pertaining to the amino-substituted species. The final concentration of the diazaquinone in the analyzing chamber was (2–8) × 10<sup>-5</sup> M. The concentration of the nucleophile was always in excess over that of the diazaquinone.

**Radiolytic Measurements.** The accelerator and the pulse radiolysis system which can be operated in three detection modes, namely absorbance, emission, and conductivity, have been described elsewhere.<sup>11–13</sup> In these experiments the concentration of the radicals initially generated was >5 × 10<sup>-5</sup> M.

Since the OH<sup>•</sup> radical, formed in the radiolysis of N<sub>2</sub>O-saturated water, adds to aromatic nuclei it was converted to N<sub>3</sub><sup>•</sup> or CO<sub>3</sub><sup>•-</sup> through the reactions



or



In this way side reactions were suppressed in favor of the one-electron oxidation of the hydrazides. In absorbance measurements the spectra observed subsequent to e<sup>-</sup>-beam irradiation correspond to the difference in extinction coefficients between the transient species and the starting material in question.

From the rate constants in Table I it can be calculated that 90% of the diazaquinone is formed within 3 × 10<sup>-4</sup> s.<sup>16</sup>

When N<sub>3</sub><sup>•</sup> was employed as oxidant, N<sub>3</sub><sup>-</sup> was always present. In studying hydrolytic mechanisms in such solutions care was taken to suppress azidolysis. Thus, the N<sub>3</sub><sup>-</sup> concentration was adjusted to comply to the condition

$$k_{\text{N}_3^-}[\text{N}_3^-] \ll k_{\text{OH}^-}[\text{OH}^-] + k_{\text{H}_2\text{O}}$$

with the rate constants taken from Table II. In the study of the azidolysis the reverse condition held, namely

$$k_{\text{N}_3^-}[\text{N}_3^-] \gg k_{\text{OH}^-}[\text{OH}^-] + k_{\text{H}_2\text{O}}$$

In order to extend the experimental time range to tens of seconds the following modifications were undertaken. In the absorbance mode a bridge was inserted by means of which the reference signal could be balanced out manually. Here, the reference signal derived from the transmitted light prior to the electron pulse. The upper time limit in these measurements was set by the photochemical deterioration of the sample by the analyzing light. In dc conductometric experiments balanced cells were used. Even so, polarization occurred due to the unavoidable slight mismatch between the cells. This shortcoming could be obviated by subtracting from the sample signal a reference signal obtained in the absence of the electron pulse. In this way the time range was extended to 10 s.

In order to expand the time scale in emission measurements the sensitivity of the light detector has to be increased since the light intensity is lessened. This was achieved by placing the P–M tube as close as 0.2 m from the sample cell. The latter was made of graphite in order to minimize the bremsstrahlung and to avoid scintillation. The P–M tube was surrounded by lead and μ-metal. Despite these precautions the electron pulse interfered with the response of the P–M tube. Fortunately, this interference proved to be reproducible; whence, correction was possible. Pulsed irradiations proved feasible for kinetic measurements on the chemiluminescence over the entire pH range. This was, however, not the case when the pH-dependence of the light yield and the end product composition was studied.

To investigate the latter in the chemiluminescent reaction of a diazaquinone with H<sub>2</sub>O<sub>2</sub> the primary oxidant employed had to fulfill the following conditions over the pH interval of interest: (1) feasibility of production and (2) a sufficiently large ratio (~100) between the rates of oxidation of the parent hydrazide and H<sub>2</sub>O<sub>2</sub>. The concentration of H<sub>2</sub>O<sub>2</sub> must be high enough to suppress any side reaction of the diazaquinone, e.g., hydrolysis, reaction with the parent hydrazide, or reaction with the anion from which the primary radical was generated (e.g., N<sub>3</sub><sup>-</sup>). Detailed study of different oxidants revealed that only ClO<sub>2</sub> fulfilled the above conditions. However, it is coproduced with HOCl in its radiolytic generation.<sup>17</sup> Therefore, prior to reacting ClO<sub>2</sub> with a hydrazide HOCl had to be removed (see below).

The light yield vs. pH measurements were made by bubbling a steady stream of ClO<sub>2</sub> in Ar through the measuring cell which was attached to the window of the P–M tube. The size of the gas–liquid contact area was smaller than the cross section of the P–M window. The cell contained 3 mL of an aqueous 10<sup>-4</sup> mol dm<sup>-3</sup> solution of the desired hydrazide. At each pH the H<sub>2</sub>O<sub>2</sub> concentration was increased until the light yield reached a stable upper limit.

ClO<sub>2</sub> was generated by irradiating 60 mL of a 1 M aqueous NaClO<sub>2</sub> solution kept at pH > 11 in a AECL<sub>220</sub>Co<sup>60</sup> γ-cell. Ar was fed continuously through the solution the high pH in the latter preventing any carry over of Cl<sub>2</sub>. The steady-state flow of ClO<sub>2</sub> entering the reaction cell was

(14) Hayon, E.; Simic, M. *J. Am. Chem. Soc.* **1970**, *92*, 7486.

(15) Ross, F., Ross, A. B., Eds.; *Natl. Stand. Ref. Data Ser.* (U.S. Natl. Bur. Stand.) NSRDS-NBS 59 (1977).

(16) All the hydrazides **3a** to **3f** undergo oxidation as monoanions. On the time scale of our experiments the neutral hydrazides were found to be unreactive toward the oxidants employed. The p*K*<sub>a</sub> values of **3a** through **3f** range between 6.7 and 7.2.

(17) Eriksen, T. E.; Lind, J.; Merenyi, G. *J. Chem. Soc., Faraday Trans. 1* **1981**, *77*, 2115.

(9) Eriksen, T. E.; Lind, J.; Merenyi, G. *J. Chem. Soc., Faraday Trans. 1* **1981**, *77*, 2125.

(10) Nikokavouras, J.; Perry, A.; Vassilopoulos, G. *Isr. J. Chem.* **1972**, *10*, 19.

(11) Rosander, S. Thesis, Royal Institute of Technology, Stockholm, 1974, TRITAEEP-74-16, p 28.

(12) Eriksen, T. E.; Lind, J.; Reitberger, T. *Chem. Scr.* **1976**, *10*, 5.

(13) Eriksen, T. E. *Chem. Scr.* **1975**, *7*, 193.

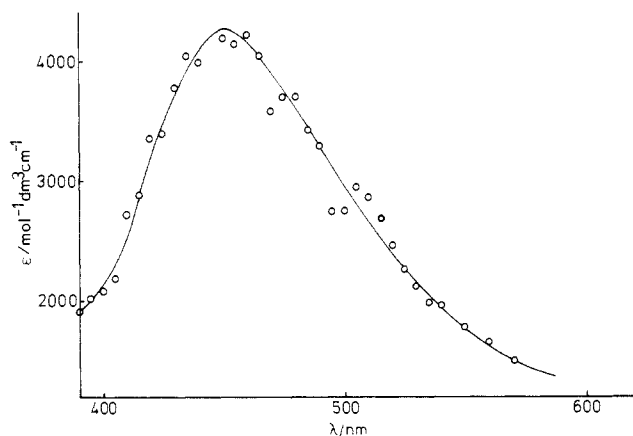


**Figure 1.** Transient optical spectrum of **2f** obtained by pulsed radiolysis of a  $\text{N}_2\text{O}$  saturated aqueous solution at pH 7 containing  $10^{-3} \text{ mol dm}^{-3}$  of 2,3-dihydrobenzophthalazine-1,4-dione (**3f**) and  $3 \times 10^{-2} \text{ mol dm}^{-3}$  of  $\text{NaN}_3$ . The dose was 100 Gy, and the spectrum was recorded 300  $\mu\text{s}$  after the electron pulse.

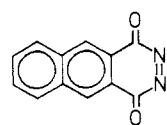
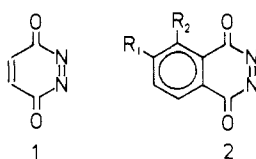
determined by iodometry to be  $5 \times 10^{-9} \text{ mol s}^{-1}$ . This amount resulted in the production of  $8 \times 10^{-7} \text{ M s}^{-1}$  diazaquinone. In all light yield and product yield experiments less than 30% of the hydrazide was consumed. Product analysis was performed by means of reversed phase HPCL.  $\text{N}_2$  was determined gas chromatographically. The total error in product analysis amounted to 10%.

**Chemicals.** The hydrazides were either purchased commercially (luminol, phthalhydrazide, EGA-Chemie) or synthesized from the corresponding phthalic acids. The hydrazides were twice recrystallized from 0.1 M KOH.  $\text{ClO}_2$  solutions were prepared from commercial  $\text{NaClO}_2$  according to ref 17. Samples were freshly prepared for each experimental series. The concentration of  $\text{ClO}_2$  was checked spectroscopically employing  $\epsilon_{360 \text{ nm}} = 1250 \text{ mol}^{-1} \text{ dm}^3 \text{ cm}^{-1}$ .

The anilines were obtained from the Department of Organic Chemistry, and they were purified (recrystallized or distilled) prior to use. All other chemicals were of p.a. quality.

## Results

**The Electronic Spectra of Diazaquinones.** The  $\pi^* \leftarrow \pi$  transition of the highest wavelength absorption in the spectra of unsubstituted diazaquinones displays a regular red-shift upon augmenting the compound with an additional fused benzene ring. Thus, the peak maxima in the homologous series **1**, **2a**, and **2f** are at 260<sup>7</sup>, 360, and 450 nm, respectively. Figure 1 displays the transient spectrum of benzophthalazine-1,4-dione (**2f**), one of the compounds studied in detail in this work.



	R <sub>1</sub>	R <sub>2</sub>
a	H	H
b	H	NH <sub>2</sub>
c	(CH <sub>3</sub> ) <sub>2</sub> N	H
d	NH <sub>2</sub>	H
e	OH	H

Phthalazine-1,4-diones substituted by electron-donating groups on the benzene ring have absorption maxima at long wavelengths which are the result of charge-transfer type transitions involving the substituent and the hetero ring. Quantum chemical calculations reflect rather accurately the nature of these transitions. The spectra of 5-amino- and 6-(dimethylamino)phthalazine-1,4-

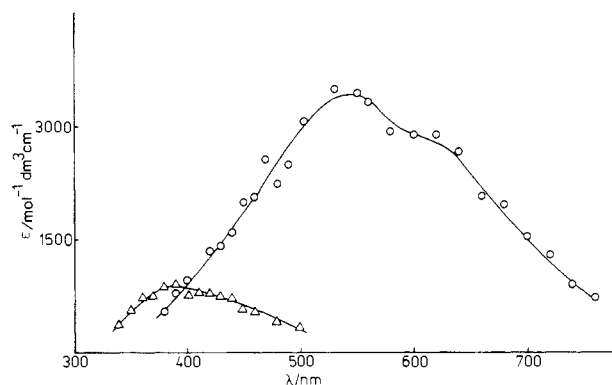


**Figure 2.** Transient optical spectra of **2e**, obtained upon the oxidation of 6-hydroxy-2,3-dihydrophthalazine-1,4-dione (**3e**) by  $\text{ClO}_2$  in stopped flow experiments: ( $\Delta$ ) spectrum obtained at pH 3; ( $\circ$ ) spectrum obtained at pH 8.

**Table III.** Activation Parameters<sup>a</sup> for the Nucleophilic Attack

nucleophile	diazaquinone					
	<b>2f</b>		<b>2b</b>		<b>2c</b>	
	$\Delta H^\ddagger$	$\Delta S^\ddagger$	$\Delta H^\ddagger$	$\Delta S^\ddagger$	$\Delta H^\ddagger$	$\Delta S^\ddagger$
$\text{H}_2\text{O}$	$34 \pm 1$	$-124 \pm 4$	$38 \pm 3$	$-125 \pm 11$	$30 \pm 4$	$-141 \pm 12$
$\text{OH}^-$	$0 \pm 2$	$-113 \pm 5$	$1 \pm 1$	$-125 \pm 6$	$0 \pm 2$	$-118 \pm 5$
$\text{H}_2\text{S}$	$0 \pm 1$	$-174 \pm 10$				
$\text{HS}^-$	$-1 \pm 2$	$-93 \pm 10$				
$\text{HO}_2^-$	$2 \pm 3$	$-96 \pm 10$	$-1 \pm 1$	$-105 \pm 10$	$0 \pm 1$	$-100 \pm 10$
$\text{CN}^-$	$23 \pm 4$	$-35 \pm 8$				
$\text{HN}_3$	$0 \pm 3$	$-148 \pm 10$				
$\text{N}_3^-$	$36 \pm 3$	$-64 \pm 11$	$26 \pm 1$	$-112 \pm 3$		
$\text{SCN}^-$	$38 \pm 5$	$-42 \pm 15$	$21 \pm 2$	$-121 \pm 5$		
$\text{I}^-$			$12 \pm 2$	$-162 \pm 10$		

<sup>a</sup>  $\Delta H^\ddagger$  in  $\text{kJ mol}^{-1}$ ;  $\Delta S^\ddagger$  in  $\text{J mol}^{-1} \text{ K}^{-1}$ .

**Table IV.** Measured Second-Order Rate Constants for the Addition of Substituted Anilines to **2b** at 25 °C in the presence of  $\sim 10^{-3}$  Phosphate Buffer at pH 7.2

substituent	$\text{p}K_a$	$k_1$ ( $\text{mol}^{-1} \text{ dm}^3 \text{ s}^{-1}$ )	$\Delta H^\ddagger$ ( $\text{kJ/mol}$ )
H	4.60	$(2.4 \pm 0.1) \times 10^4$	
4- $\text{SO}_3^-$	3.22	$(6.1 \pm 0.4) \times 10^1$	$10 \pm 6$
4- $\text{CO}_2^-$		$(1.8 \pm 0.2) \times 10^2$	
4-F	4.60	$(3.5 \pm 0.1) \times 10^3$	$9 \pm 3$
4- $\text{CH}_3$	5.10	$(2.2 \pm 0.2) \times 10^4$	$10 \pm 4$
4- $\text{OCH}_3$	5.34	$(3.7 \pm 0.1) \times 10^5$	$4 \pm 6$
4-OH	5.65	$(7.0 \pm 0.8) \times 10^6$	
3-Br	3.54	$(1.6 \pm 0.1) \times 10^3$	
3- $\text{OCH}_3$	4.21	$(2.9 \pm 0.2) \times 10^6$	
2-Br	2.53	$(7.5 \pm 0.5) \times 10^2$	
2- $\text{CH}_3$	4.45	$(1.8 \pm 0.1) \times 10^5$	
2,6- $(\text{CH}_3)_2$	3.89	$(1.6 \pm 0.2) \times 10^6$	
2,6- $(\text{C}_2\text{H}_5)_2$		$(1.7 \pm 0.1) \times 10^6$	
<i>N</i> - $\text{CH}_3$	4.85	$(5.5 \pm 0.1) \times 10^5$	
<i>N,N</i> - $(\text{CH}_3)_2$	5.10	$(8.2 \pm 0.4) \times 10^5$	

diones (**2b** and **2c**) have broad absorptions centered around 560<sup>9</sup> and 600 nm, respectively. Figure 2 demonstrates the marked difference between the spectra of neutral and anionic **2e**. The drastic red-shift and the increase in oscillator strength owing to the dissociation of the phenolic OH group support the charge-transfer character of the spectral transition.

**The Nucleophilic Attack.** Throughout this work the rate constant with any particular nucleophile was measured by observing the disappearance of the characteristic absorbance of the diazaquinone. The second-order rate constants were obtained from least-square fits of the observed rates vs. nucleophile concentration. At least five concentrations of the nucleophile were employed and at each concentration an average of six measurements were made. This procedure was repeated at each temperature for the establishment of the activation parameters. Table II contains the rate constants of various nucleophiles with the diazaquinones **2f**, **2b**, and **2c**. In some cases the rate constants with species **2a** were

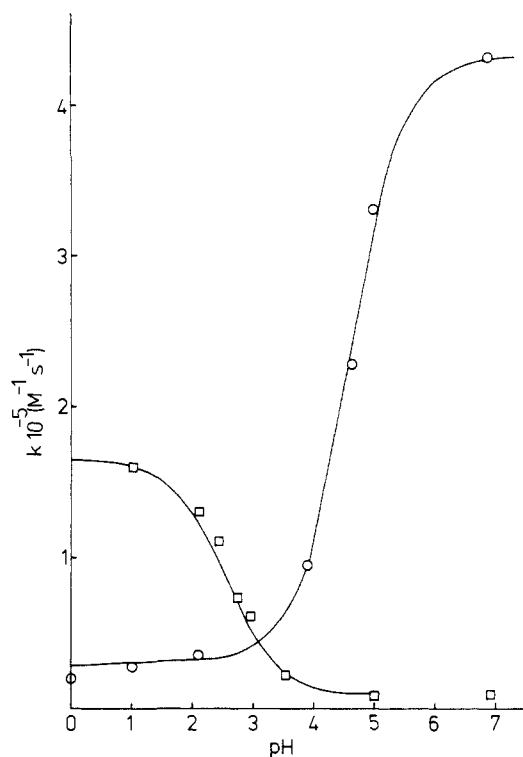


**Figure 3.** pH dependence of the rate constants of addition of (O) aniline and (□) *o*-bromoaniline to **2f**. The titration curves are best fits to the experimental points by use of the  $pK_A$  values of aniline (4.60) and *o*-bromoaniline (2.58).

also measured. Table III presents the activation parameters for some of the above reactions. In order to investigate substituent effects on the nucleophilic attack a series of substituted anilines were employed. The measured rate constants are displayed in Table IV. For some anilines (see Table IV) the nucleophilic attack rates on species **2b** were measured at a few temperatures. From these the reported activation enthalpies were estimated.

In Figure 3 the effect of pH on the rate of attack on species **2f** is demonstrated for aniline and *o*-bromoaniline. Note the increased rate of the latter upon protonation.

The rate of attack of *p*-fluoroaniline on species **2b** was enhanced by various buffers. Four different buffer systems each consisting of an equimolar mixture of the conjugate acid–base pair were investigated. These were formate ( $\text{HCOOH}/\text{HCO}_2^-$ ), acetate ( $\text{CH}_3\text{COOH}/\text{CH}_3\text{CO}_2^-$ ), maleate ( $\text{C}_4\text{O}_4\text{H}_3^-/\text{C}_4\text{O}_4\text{H}_2^{2-}$ ) and phosphate ( $\text{H}_2\text{PO}_4^-/\text{HPO}_4^{2-}$ ). The rate of disappearance of **2b** initially formed ( $3 \times 10^{-4}$  M) was measured at constant 4-fluoroaniline concentration ( $2.5 \times 10^{-3}$  M) as a function of the buffer concentration where the pH of the solution corresponded to the  $pK_A$  of the particular acid–base pair employed. Control experiments at certain buffer concentrations showed that the measured rate was always first order in the aniline. With the above acid–base pairs the following third-order rate constants ( $\text{M}^{-2} \text{s}^{-1}$ ) as calculated per total buffer concentration were obtained: ( $5 \pm 9$ )  $\times 10^3$  (formate), ( $1.8 \pm 0.2$ )  $\times 10^4$  (acetate), ( $2.9 \pm 0.1$ )  $\times 10^4$  (maleate), and ( $7.6 \pm 0.4$ )  $\times 10^4$  (phosphate). Since the above rate constants increase with increasing  $pK_A$  of the acid–base pair, it is clear that a general base catalysis is operating. Note in particular that within experimental accuracy formate has no effect. Since the latter is studied at pH 3.75 where 4-fluoroaniline is almost completely protonated, it appears that the addition of the conjugate acid is an uncatalyzed reaction. The intercepts of rate vs. buffer concentration plots correspond to the uncatalyzed rate constant at the working pH. After correction for the hydrolysis rate we obtain from them the second-order rate constants ( $\text{M}^{-1} \text{s}^{-1}$ ) for the uncatalyzed addition of 4-fluoroaniline to **2b** to be  $9 \times 10^3$  (pH 3.75),  $5 \times 10^3$  (pH 4.75),  $3.5 \times 10^3$  (pH 6.1), and  $3.5 \times 10^3$  (pH 7.2). The last two values agree with the one presented in Table IV where the rate constant was determined

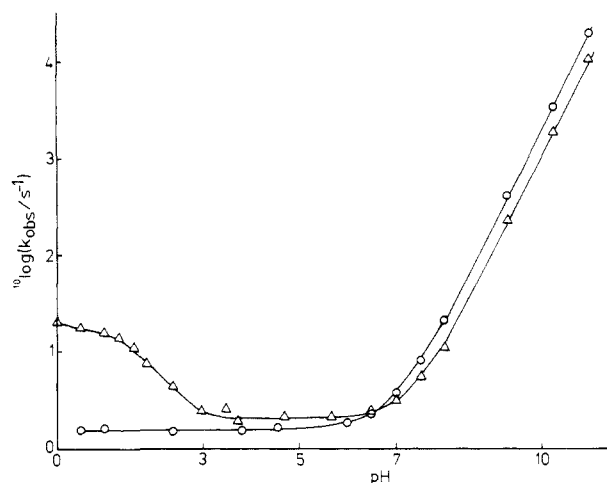


**Figure 4.** pH dependence of the rate constants of hydrolysis. Between pH 0 and 8 the values were measured by stopped flow while above pH 8 pulse radiolysis was utilized: (O) compound **2f**, measured at 470 nm; ( $\Delta$ ) **2c**, measured at 600 nm.

from rate vs. aniline concentration plots at buffer concentrations ( $\sim 10^{-3}$  M) where the catalytic effect was negligible. Note that at pH 3.75 where 4-fluoroaniline is mostly protonated the rate constant is higher than for the neutral aniline. This is similar to the observation made for the addition of 2-bromoaniline to **2f**.

Since all rate constants were measured in water where the lowest rate of hydrolysis of **2b**, **2c**, and **2f** is about  $1 \text{ s}^{-1}$  (see Table II), only those nucleophiles could be studied for which  $k_{\text{obsd}} [\text{Nu}^-]_{\text{tot}} > 1 \text{ s}^{-1}$  held under realistic experimental conditions. This precluded the halogenides except  $\text{I}^-$  and a detailed study of the aliphatic amines. The latter had to be studied at concentrations of up to 1 M around pH 7 where most of the amine is protonated. The reported rate constants are based on the amount of neutral amine present as derived from the  $pK_A$  values 9.25 and 10.8 for  $\text{NH}_4^+$  and  $\text{C}_2\text{H}_5\text{NH}_3^+$ , respectively.

The rate of hydrolysis was investigated in the entire pH interval 0–14. The pH dependence of the hydrolysis rates of species **2c** and **2f** are presented in Figure 4. As can be seen, the two curves are very similar except for the increase of the hydrolysis rate of **2c** below pH 3. The latter is probably due to the protonation of the dimethylamino group. Above pH 3 both compounds display a pH independent region up to about pH 7 followed by an  $\text{OH}^-$ -catalyzed regime. For the neutral hydrolysis of **2f** the solvent kinetic isotope effect  $k_{\text{H}_2\text{O}}/k_{\text{D}_2\text{O}}$  was found to be  $3.0 \pm 0.1$ . A slight effect of the buffer concentration on the hydrolysis reaction was observed. For compound **2f** phosphate at pH 6.9 had the maximum effect, the rate constant as calculated per total phosphate being  $3 \text{ mol}^{-1} \text{ dm}^3 \text{ s}^{-1}$ . The effect of pH on the attacks of  $\text{N}_3^-$ ,  $\text{SCN}^-$ ,  $\text{SH}^-$ ,  $\text{CN}^-$ , and  $\text{HO}_2^-$  on species **2f** was studied below pH 8.  $\text{SH}^-$ ,  $\text{CN}^-$ , and  $\text{HO}_2^-$  have nucleophilic rate constants which decrease with decreasing pH reflecting the protonation of the anion to attain the rate due exclusively to the conjugate acid. The rate constants of the anions were evaluated from the pH dependence and the respective  $pK_a$  values. Due to the high  $pK_a$  of  $\text{H}_2\text{O}$  and  $\text{H}_2\text{O}_2$  accurate determination of the rate constant of the  $\text{OH}^-$  and  $\text{HO}_2^-$  attacks required measurements above pH 8. This was accomplished by means of pulse radiolysis, according to ref 9 and 18. In determining the activation parameters for  $\text{OH}^-$ ,  $\text{CN}^-$ ,  $\text{SH}^-$ , and  $\text{HO}_2^-$  allowance was made for the temperature dependences of the pH of the buffer solution, the  $pK_w$  and the  $pK_a$  values of  $\text{HCN}$ ,<sup>19</sup>  $\text{H}_2\text{S}$ ,<sup>20</sup> and  $\text{H}_2\text{O}_2$ ,<sup>21</sup> respectively. In contrast to  $\text{SH}^-$ ,  $\text{CN}^-$ , and  $\text{HO}_2^-$ , both  $\text{N}_3^-$  and  $\text{SCN}^-$  displayed increasing reactivity upon

(18) Eriksen, T. E.; Lind, J.; Merenyi, G. *J. Chem. Soc., Faraday Trans. 1*, **1981**, *77*, 2137.

(19) Izatt, R. M.; Christensen, J. J.; Pach, R. T.; Bench, R. *Inorg. Chem.* **1962**, *1*, 828.

(20) Wright, R. H.; Maas, O. *Can. J. Res.* **1932**, *6*, 588.

(21) Joyner, R. A. *Z. Anorg. Chem.* **1912**, *77*, 103.

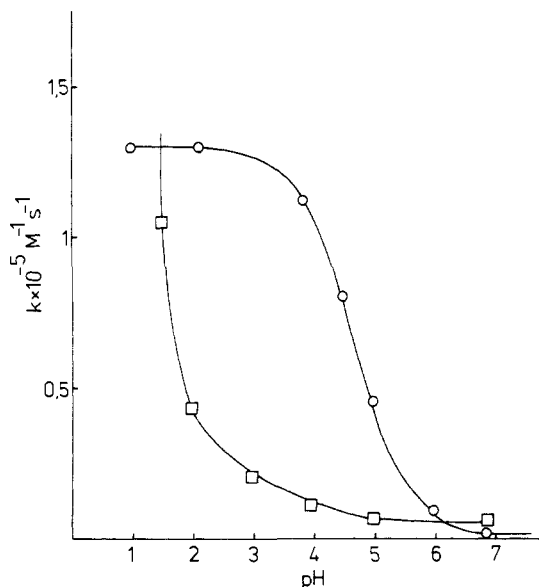


**Figure 5.** pH dependence of the rate constants of addition of (○)  $\text{N}_3^-$  and (□)  $\text{SCN}^-$  to **2f**. The titration curve for  $\text{N}_3^-$  is a best fit to the experimental points by use of the  $\text{p}K_A$  of  $\text{HN}_3$  (4.68).

lowering the pH (see Figure 5).

At pH 7, phosphate increases the rate of  $\text{N}_3^-$  attack on **2f**. A threefold increase is calculated at 1 M phosphate which is similar to the effect found for the hydrolysis of **2f**.

**Subsequent Reactions.** From the multitude of the nucleophiles employed we have chosen  $\text{N}_3^-$ ,  $\text{OH}^-$ , and  $\text{HO}_2^-$  for the study of the entire reaction sequence leading to end products. Other nucleophiles were considered only cursorily.

Subsequent to the initial reaction of  $\text{OH}^-$  or  $\text{N}_3^-$  further spectral changes were observed at shorter wavelengths with all the diazaquinones studied. Thus, simultaneously with the decay of the absorbance of species **2a** at 360 nm a new absorbance arose around 270 nm. Similarly, the absorbance of **2c** at 600 nm vanished to give rise to an absorbance around 370 nm (see Figure 6). The new absorbances deriving from **2a** and **2c** underwent further spectral changes with time. As will be shown below these spectra are due to acyl diazene species (see Schemes III and V).

**The Hydrolysis.** The absorbance at 270 nm (due to the hydrolysis of **2a**) was found to decay with a pH-dependent first-order rate constant (see Figure 7). The curve in Figure 7 is a least-square fit of the equation  $k_0 + k_1 [\text{OH}^-]$  to the experimental points. The values obtained for  $k_0$  and  $k_1$  are  $0.12 \text{ s}^{-1}$  and  $5.6 \times 10^3 \text{ M}^{-1} \text{ s}^{-1}$ , respectively. A typical kinetic trace is shown in Figure 8C.

After the decay of the absorbance at 270 nm no further change in absorbance could be detected. Within experimental error the final spectrum corrected for the consumption of phthalic hydrazide (**3a**) coincided with that of 2-formyl benzoate (**11a**). Product analysis on irradiated phthalic hydrazide solutions at pH 6.5, 9.3, 10.6, and 12 gave identical product yields consisting of more than 90% **11a**, the remainder being phthalate (**12a**). The yields are based on **2a** initially formed.

The change in absorbance around 370 nm (due to the hydrolysis product of **2c**) reveals a reaction pattern which depends on the pH and the initial concentration of **2c**. Actually due to the nonequivalence of the carbonyl groups in **2c** two isomers of **10c** are expected. However, only the isomer possessing a carbonyl group in a para position to the amino group should absorb substantially above 350 nm judging from the spectral characteristics of analogous substances. Below pH 11 the absorbance decayed with a first-order rate constant fitting the expression (see Figure 9)

$$k_{\text{obsd}} = (7 \times 10^{-4}) + (5 \times 10^3)[\text{OH}^-] \text{ (s}^{-1}\text{)}$$

Above pH 11 two kinetic steps were observed, the first one giving rise to a slight red-shift in the spectrum (see Figure 6). This

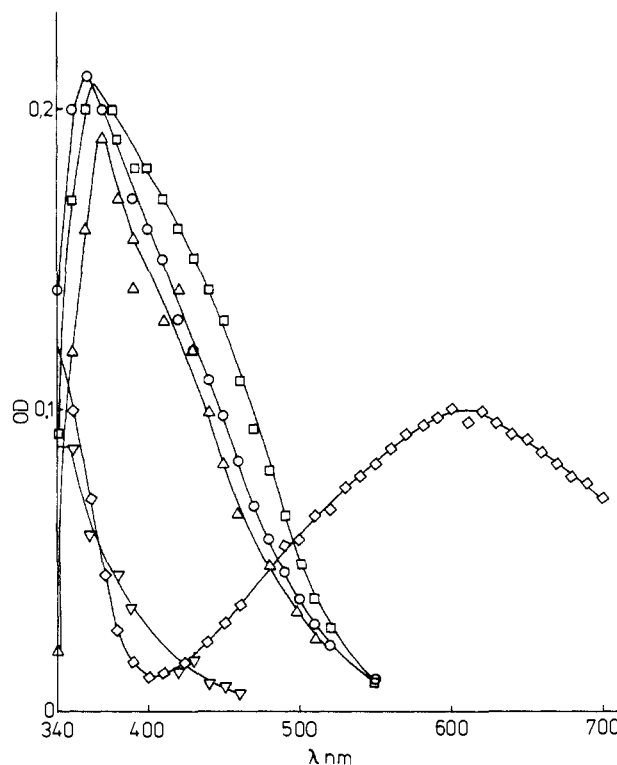


**Figure 6.** Transient spectra obtained upon pulsed radiolysis of  $\text{N}_2\text{O}$ -saturated aqueous solutions containing  $2 \cdot 10^{-4} \text{ mol dm}^{-3}$  of 6-(dimethylamino)-2,3-dihydrophthalazine-1,4-dione (**3c**). The dose per pulse was 300 Gy: (◇) transient spectrum of **2c** obtained at pH 7.35 in the presence of  $5 \times 10^{-3} \text{ mol dm}^{-3}$  of  $\text{NaN}_3$  and recorded 300  $\mu\text{s}$  after the end of the pulse; (Δ) transient spectrum of **13c** recorded 20 ms after the end of the pulse in the presence of  $0.5 \text{ mol dm}^{-3}$  of  $\text{NaN}_3$  at pH 7.35. (○) transient spectrum of **10c** (trans) recorded 300  $\mu\text{s}$  after the end of the pulse in the presence of  $5 \times 10^{-3} \text{ mol dm}^{-3}$  of  $\text{NaN}_3$  at pH 12. (□) transient spectrum of **10c** (cis) recorded 40 ms after the end of the pulse in the presence of  $5 \times 10^{-3} \text{ mol dm}^{-3}$  of  $\text{NaN}_3$  at pH 12. (▽) final spectrum recorded 2 s after the end of the pulse in the presence of  $5 \times 10^{-3} \text{ mol dm}^{-3}$  of  $\text{NaN}_3$  at pH 12. Note that with the  $\text{OH}^-$  and  $\text{N}_3^-$  concentrations employed **2c** is converted to azidolyzed (Δ) or hydrolyzed (○, □, ▽) species. (For a discussion of the concentration dependence see Experimental Section).

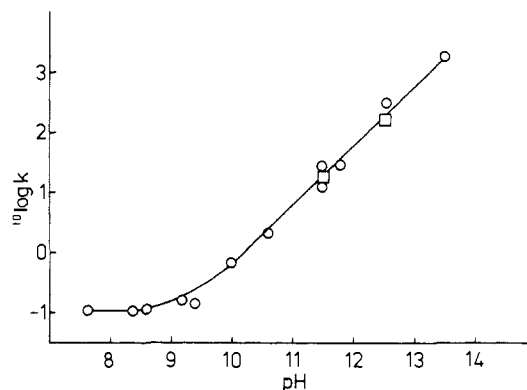


**Figure 7.** pH dependence of the hydrolysis rate of **10a** measured at 270 nm: (○) **10a** obtained through the hydrolysis of **2a**; (□) **10a** obtained through the two-electron oxidation of species **6**. The curve is described in the text.

transformation was only  $\text{OH}^-$  dependent with  $k_{\text{OH}^-} = 5 \times 10^3 \text{ M}^{-1} \text{ s}^{-1}$  which is identical with the  $\text{OH}^-$  dependent rate constant found at lower pH. Note, however, that while the spectral transformation at  $\text{pH} > 11$  was only slight the low pH equivalent was a drastic decrease of the absorbance (see Figure 6). Above pH 11 the first-order step giving rise to the red-shift was followed by a second process which manifested itself as a substantial decay of the absorbance. Between pH 11 and 12.5 the rate of the latter de-

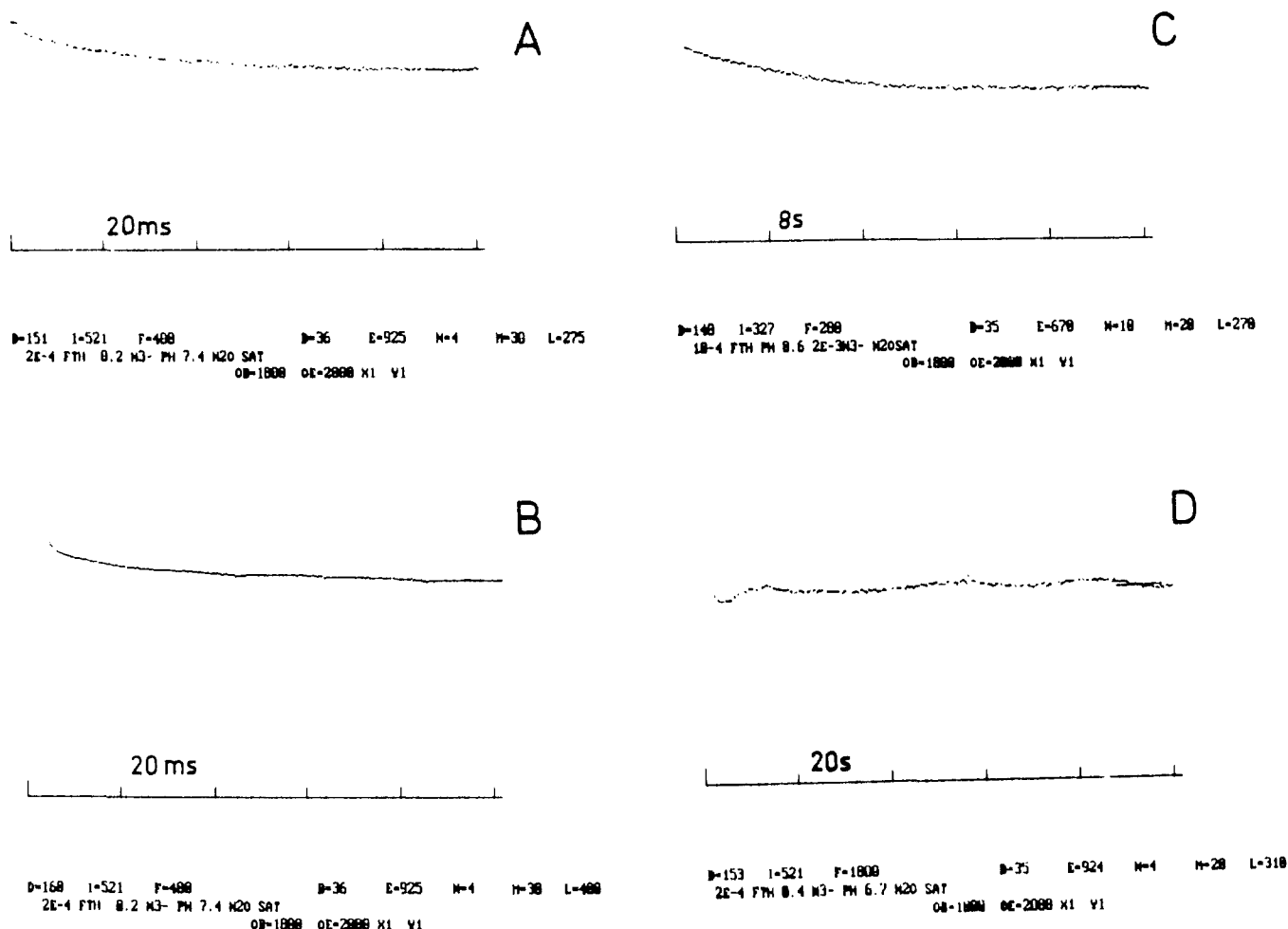


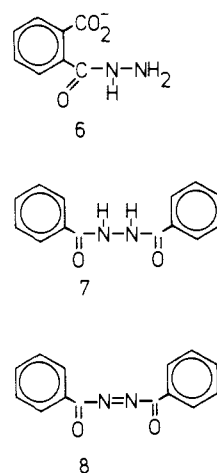
**Figure 8.** Kinetic traces obtained upon pulsed radiolysis of  $\text{N}_2\text{O}$ -saturated aqueous solutions containing species **3a**: (a)  $2 \times 10^{-4}$  mol  $\text{dm}^{-3}$  of **3a**,  $0.2$  mol  $\text{dm}^{-3}$  of  $\text{NaN}_3$ , pH 7.4. The trace was recorded at 275 nm. (b)  $2 \times 10^{-4}$  mol  $\text{dm}^{-3}$  of **3a**,  $0.2$  mol  $\text{dm}^{-3}$  of  $\text{NaN}_3$ , pH 7.4. The trace was recorded at 400 nm. (c)  $10^{-4}$  mol  $\text{dm}^{-3}$  of **3a**,  $2 \times 10^{-3}$  mol  $\text{dm}^{-3}$  of  $\text{NaN}_3$ , pH 8.6. The trace was recorded at 270 nm. (d)  $2 \times 10^{-4}$  mol  $\text{dm}^{-3}$  of **3a**,  $0.4$  mol  $\text{dm}^{-3}$  of  $\text{NaN}_3$ , pH 6.7. The trace was recorded at 310 nm. The first 10 s of trace d describe two kinetic steps characterized by a bleaching and a buildup of the absorbance, while the remainder of the trace demonstrates the fluctuation of the base line. Note that trace c depicts hydrolysis while the other traces refer to azidolysis (see Experimental Section).

pended on the initial concentration of **2c** but not on the pH (see insert in Figure 9). From this decay a second-order rate constant  $2k \approx 10^5 \text{ M}^{-1} \text{ s}^{-1}$  was estimated. Above pH 12.5 this decay was  $\text{OH}^-$  dependent but almost independent on the initial concentration of **2c**. The rate constant for the  $\text{OH}^-$  induced reaction was found to be  $k_{\text{OH}^-} = 30 \text{ M}^{-1} \text{ s}^{-1}$ . In some control experiments the non-methylated analogue, **2d**, revealed the same qualitative behavior as **2c** with similar rate constants.

The absorbance studies on **2a** and **2c** were complemented by pulsed conductimetric measurements. Unbuffered and  $\text{N}_2\text{O}$  saturated solutions at pH 9.8 and 10.7 containing  $2 \times 10^{-4}$  **3a** or **3c** and  $10^{-3}$  M  $\text{NaN}_3$  were irradiated by  $e^-$ -beam pulses, generating radical concentrations  $\sim 10^{-4}$  mol/ $\text{dm}^3$ . In aqueous solutions the predominant changes in conductivity are due to pH shifts. Above pH 7 the formation of  $\text{OH}^-$  increases the conductivity while the reverse is true for its consumption. After radical dismutation, i.e., once **2a** or **2c** have formed, the conductivity in these experiments decreased in a first-order process, the rate being equal to the attack of  $\text{OH}^-$  on **2a** or **2c** as was confirmed by absorbance measurements on identical solutions. Thus, charge conservation demands the formation of a monoanion simultaneously with the consumption of  $\text{OH}^-$ . No further changes in conductivity could be observed over 10 s. Thus it follows that no net change of protons is involved in the first-order processes following hydrolysis of **2a** or **2c**.

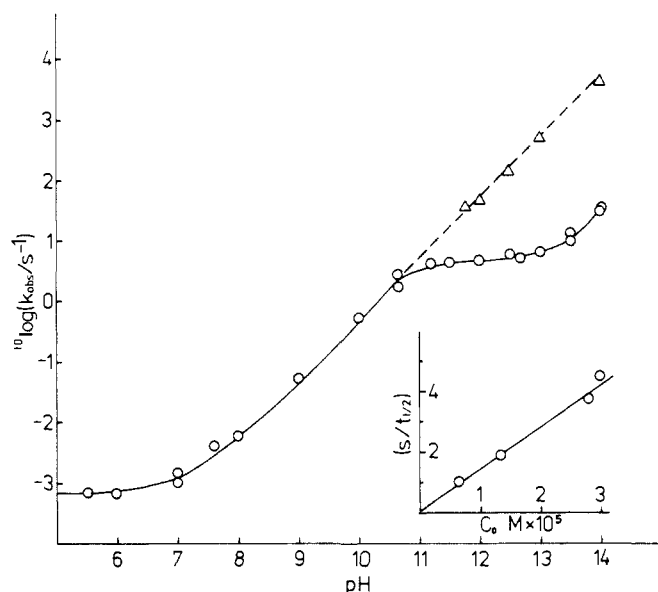
The two-electron oxidation of **6** is expected to yield the intermediate **10a** observed in the hydrolysis of **2a**. Indeed a transient appears with an absorbance around 270 nm. The rate of its disappearance agrees quantitatively with the values presented in

Figure 7. In a similar experiment the oxidation of **7** yields an azo species **8** absorbing around 400 nm which hydrolyses ( $k_{\text{obsd}}$



$= k[\text{OH}^-]$ ,  $k = 5 \times 10^3 \text{ M}^{-1} \text{ s}^{-1}$ ) to form a species absorbing at 270 nm. The latter undergoes further hydrolysis, the rate constant of its alkaline hydrolysis ( $k \approx 2 \times 10^3 \text{ M}^{-1} \text{ s}^{-1}$ ) being close to the values in Figure 7.

**The Azidolysis.** Pulsed radiolysis in the pH interval 6.5–7.5 was performed on  $\text{N}_2\text{O}$  saturated solutions containing  $2 \times 10^{-4}$  M phthalic hydrazide and varying concentrations of  $\text{NaN}_3$ . The absorbance of **2a** at 360 nm decayed with a rate proportional to



**Figure 9.** pH dependence of the hydrolysis rate of **10c**. Above pH 10 the values were obtained upon pulsed radiolysis of  $N_2O$ -saturated aqueous solutions containing  $10^{-4}$  mol  $dm^{-3}$  of compound **3c** and  $2 \times 10^{-3}$  mol  $dm^{-3}$  of  $NaN_3$ . The dose per pulse was 300 Gy. Below pH 10 the values were obtained in stopped flow experiments upon oxidizing **3c** to **2c** by  $ClO_2$ . The measurements were made at 410 nm: ( $\Delta$ ) first-order transient rearrangement ( $\circ \rightarrow \square$  in Figure 6); ( $\circ$ ) decay to the final spectrum. ( $\circ \rightarrow \nabla$  or  $\square \rightarrow \nabla$  in Figure 6). Inset: the inverse of the half-life of decay vs. the initial concentration of **2c** at pH 12.5.

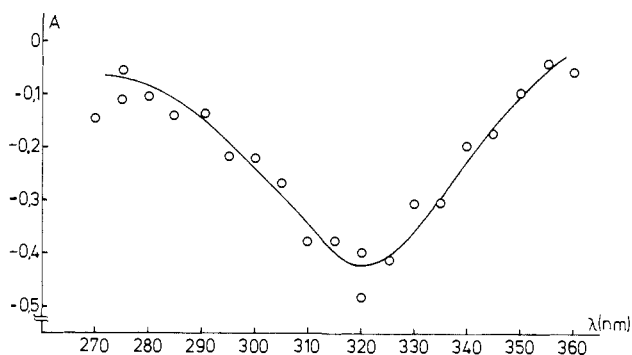


**Figure 10.** Final spectrum recorded 12 s after the delivery of 300 Gy  $e^-$  beam pulses to a  $N_2O$ -saturated aqueous solution at pH 7.35 containing  $2 \times 10^{-4}$  mol  $dm^{-3}$  of compound **3a** and  $0.5$  mol  $dm^{-3}$  of  $NaN_3$ . The curve which is described by  $\epsilon(\text{phthalimide}) - \epsilon(\mathbf{3a})$  is scaled to fit the experimental points.

the azide concentration. Concomitant with this decay a new species appeared displaying an absorbance around 270 nm. Subsequently, we observed three consecutive first-order processes (see Figure 8 (parts A, B, and D)), the first of them being characterized by a decrease of the absorbance at 270 nm. The rate of this reaction was proportional to the  $N_3^-$  and  $H^+$  concentrations in the above pH range. From these data the second-order rate constants for the reactions of  $N_3^-$  and  $HN_3$  with the intermediate were estimated to be  $50$  and  $7 \times 10^4$   $M^{-1} s^{-1}$ , respectively.

The second and third steps were observed as a decrease followed by an increase of the absorbance at 310 nm (see Figure 8D). Both reactions were unaffected by  $[N_3^-]$  and  $[H^+]$ . The first-order rate constants describing the decay ( $0.5$   $s^{-1}$ ) and the buildup ( $0.1$   $s^{-1}$ ) were extracted from a least-squares fit of the trace in Figure 8D to the sum of two exponentials.

Allowing for the bleaching of phthalic hydrazide the spectrum resulting from the last reaction was that of phthalimide (Figure 10). HPLC analysis on spent solutions identified phthalimide as the only product with a yield of  $100 \pm 10\%$  based on **2a** initially formed. To investigate the effect of pH on the product yield, species **2a**, generated in the stopped flow equipment, was mixed

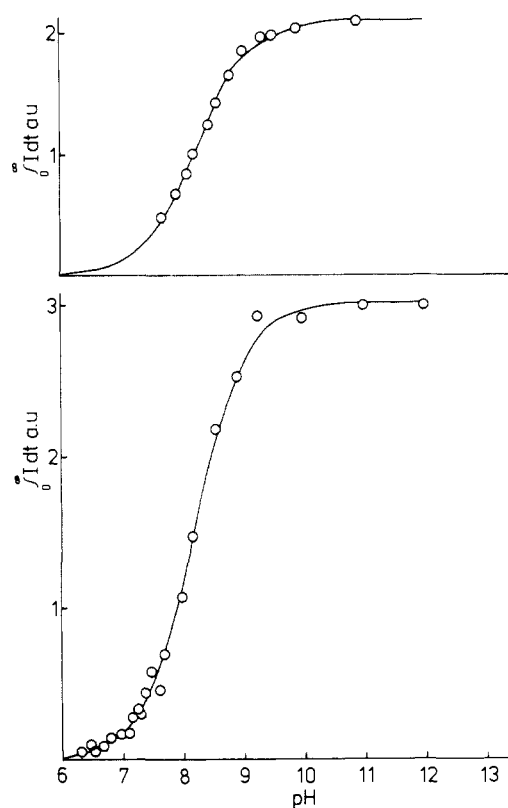


**Figure 11.** pH dependence of the maximum chemiluminescence light yield obtained upon reacting  $10^{-4}$  mol  $dm^{-3}$  of **3f** (upper figure) or **3b** (lower figure) with a steady stream of  $ClO_2$  which generates  $8 \times 10^{-7}$  mol  $dm^{-3} s^{-1}$  of the corresponding diazaquinone. The  $H_2O_2$  concentration is adjusted at each pH to obtain the maximum light. The titration curves are best fits to the experimental points. The scales of the upper and lower figures are not interrelated.

with  $N_3^-$  and  $HN_3$  at pH 7 and 2, respectively. HPLC analysis of the reaction mixtures showed that irrespective of the pH phthalimide was formed quantitatively. Azidolysis of **2c** produced species absorbing around 370 nm (see Figure 6). Contrary to the hydrolysis both of the possible  $N_3^-$  adducts **13c** are expected to absorb similarly as both of them should contain a carbonyl group in para position to the amino group. The decay rate of the absorbance of **13c** was found to be proportional to  $[N_3^-]$  at pH 7.4, but varied with the wavelength. Two individual second-order rate constants with the values  $3$   $M^{-1} s^{-1}$  (330–360 nm) and  $20$   $M^{-1} s^{-1}$  (420–470 nm) were found. The existence of two  $N_3^-$  dependent rates is thus consistent with the presence of two isomers. These values are distinctly lower than that obtained for **13a** at the same pH ( $250$   $M^{-1} s^{-1}$ ). Similarly to the case of **2a** several slow  $N_3^-$  independent reactions were observed after the completion of the  $N_3^-$  attacks. We did not attempt to assign these reactions (with rates between  $0.1$  and  $0.5$   $s^{-1}$ ) to the different isomers.

**Some Other Nucleophiles.** Stopped flow experiments showed that the attack of  $I^-$  on **2b** resulted in the formation of  $I_3^-$  and **3b** (luminol). In the case of the anilines only their initial addition to **2b** could be observed, resulting in the appearance of products absorbing around 400 nm. Gas analysis revealed no net formation of molecular  $N_2$  in the reaction of aniline or luminol with **2b**.

**$H_2O_2$  Addition and Chemiluminescence.** The addition of  $H_2O_2$  to **2f**, **2b**, and **2c** gives rise to chemiluminescence. By observing the pH dependence of the chemiluminescent kinetics and of the total light yield further insight into the nucleophilic addition could be gained. Such studies have been published by us before,<sup>18,22</sup> but an improvement in experimental technique has enabled us to study low light intensities due to the reactions of **2b** below pH 8.5. The rather weak chemiluminescence of **2f** became also

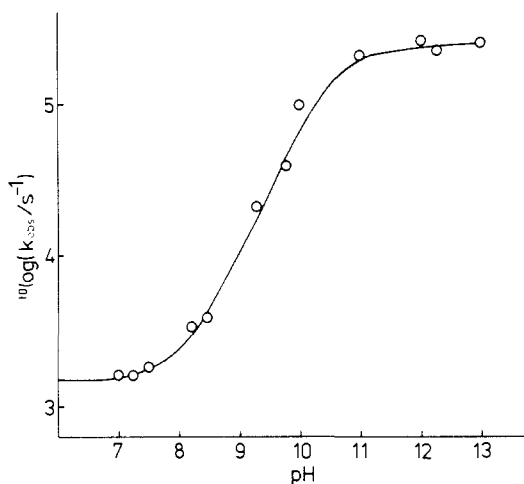
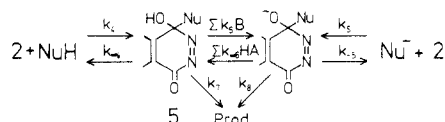


**Figure 12.** pH dependence of the first-order chemiluminescent buildup. The titration curve which corresponds to a  $pK_A = 10.4$  is a best fit to the experimental points. The values were obtained upon pulsed radiolysis of  $N_2O$ -saturated aqueous solutions containing  $2 \times 10^{-3} \text{ mol dm}^{-3}$  of luminol (**3b**),  $0.04 \text{ mol dm}^{-3}$  of  $NaN_3$ , and  $0.1\text{--}1.0 \text{ mol dm}^{-3}$  of  $H_2O_2$  (below pH  $\sim 9.5$ ) or  $O_2$ -saturated solutions containing  $10^{-3} \text{ mol dm}^{-3}$  of **3b** and  $0.1 \text{ mol dm}^{-3}$  of  $NaN_3$  (above pH  $\sim 9.5$ ).

amenable to study. The pH profiles of the total light yield of **2b** and **2f** are presented in Figure 11. Both substances display almost the same pH profile with a  $pK_A \sim 8.2 \pm 0.1$ . Product analysis performed on luminol (**3b**) solutions utilized in the light titration revealed 3-aminophthalate as the sole product, its yield per **2b** initially present increasing from  $\sim 50\%$  to  $\sim 80\%$  when the pH was lowered from 10 to 6.6. The remainder of **2b** formed **3b** and  $O_2$ . In contrast, compounds **2a** and **2f** were found to react with  $H_2O_2$  to yield quantitatively the corresponding phthalates irrespective of the pH. It may be noticed that the present  $pK_A$  of  $\int_0^\infty I dt$  lies one pH unit lower than that reported previously.<sup>22</sup> In our earlier experiments the recombination of  $O_2^{\cdot-}$  with the radical anion **4b** was utilized in the pH studies. This reaction is stoichiometrically equivalent to the addition of  $H_2O_2$  ( $HO_2^-$ ) to **2b**. At pH values above 10 the light yield and the kinetics observed for these two reactions are equal.<sup>22</sup> However, we have found that neutral **4b** reacts 31 times faster with  $O_2^{\cdot-}$  than its monoanion. From this factor and the  $pK_A = 7.7^{23}$  of **4b** it follows that at pH 9.2  $O_2^{\cdot-}$  reacts equally fast with neutral **4b** and its monoanion. This pH value coincides with the experimental  $pK_A$  of the light yield found previously. Thus we conclude that neutral **4b** reacts with  $O_2^{\cdot-}$  by electron transfer to yield  $O_2$  and **3b** while chemiluminescence requires the formation of an adduct generated in the reaction between the anion of **4b** and  $O_2^{\cdot-}$ .

Chemiluminescence traces obtained upon pulsed irradiation of luminol in the presence of  $H_2O_2$  consisted of a buildup and a decay portion. The rate of the decay at any pH was proportional to the  $H_2O_2$  concentration and yielded the rate constant for **2b** +  $HO_2^-$  (see Table II) whereas the buildup depended only on the pH as shown in Figure 12. Previously, we had determined the activation parameters of the rate constant pertaining to the high pH limit of the chemiluminescent buildup ( $\Delta H^* = 44 \text{ kJ/mol}$ ,  $\Delta S = 7 \text{ J/(mol K)}$ ).<sup>22</sup> In the present work the activation parameters for the low pH limit were determined to be  $\Delta H^* = 25 \pm 4 \text{ kJ/mol}$  and  $\Delta S = -104 \pm 5 \text{ J/(mol K)}$ . The rate measurements in the present work owe much to the increased sensitivity of detection. In light of our present insight we conclude that previous rate measurements at pH values below 9 mainly reflected the radical recombination. In pulse radiolysis experiments on solutions containing **3f** and  $O_2$  we have also determined the rate constant of the chemiluminescence buildup at pH  $> 11$  to be  $(1.3 \pm 0.5) \times 10^5 \text{ s}^{-1}$ .

## Scheme II



## Discussion

**The Initial Addition.** The diazaquinones are formally derivatives of carboxylic acids and should thus follow the same pattern as the latter with regard to nucleophilic addition (Scheme II). Nucleophilic addition to a carbonyl carbon is inferred from the simple kinetic pattern leading to the end products in the reaction of **2** with  $OH^-$  and  $N_3^-$  (see below). Since upon the addition of  $HO_2^-$  to **2** we observe an intermediate which almost certainly is tetrahedral (vide infra), it is reasonable to assume that even the addition of other nucleophiles will engender tetrahedral intermediates.

We observe that the measured rate constants for the addition of  $OH^-$ ,  $HO_2^-$ , and  $SH^-$  (see Table II) are high ( $10^6\text{--}10^8 \text{ M}^{-1} \text{ s}^{-1}$ ) and also display no activation energy. Since these anions are poor leaving groups we expect that for them  $k_5 \gg k_{-5}$  (Scheme II), i.e., the experimental rate constant is that of the forward reaction ( $k_5$ ). Within this model the nucleophilic addition occurs with no barrier.

As a further extension of the model we assume that the addition of all the anions studied occurs without activation energy and has similar rate constants ( $10^6\text{--}10^8 \text{ M}^{-1} \text{ s}^{-1}$ ). As an example we will use the addition of  $N_3^-$  to **2f**. The measured rate constant is at least a 1000-fold lower than the high rate observed for  $OH^-$ . Within the assumed model this implies that for  $N_3^-$   $k_{-5} \gg k_5$  and  $k_{-5} \gg k_8 + \Sigma k_{-6}HA$ . As long as  $pK_A(HN_3) < pH < pK_A(5)$  steady-state treatment of the tetrahedral intermediate yields eq 1

$$k_{\text{obsd}} = \frac{k_5}{k_{-5}} (k_8 + \Sigma k_{-6}HA) = K_5(k_8 + \Sigma k_{-6}HA) \approx K_5 k_x \quad (1)$$

where  $k_x$  is the dominant term in the parentheses. From the assumption of  $(\Delta H)_{-5}^* \approx 0$  it follows that

$$(\Delta H)_{\text{obsd}}^* \approx (\Delta H)_x^* - (\Delta H)_{-5}^* \quad (2)$$

The maximum value of  $k_x \approx 10^7 \text{ s}^{-1}$  is obtained by setting  $(\Delta H)_{-5}^* = 0$  and assuming a maximum frequency factor of about  $10^{13} \text{ s}^{-1}$  for  $k_x$ , i.e.,  $(\Delta S)_x^* \approx 0$ .

Scheme II rationalizes the observed activation energies and predicts reasonable values for the involved rate constants. It is, of course, conceivable that in some cases the lifetime of the tetrahedral intermediate becomes so short that it ceases to exist. Then the reaction will become an enforced concerted substitution.

In contrast to  $N_3^-$  the addition of  $HN_3$  proceeds with no activation enthalpy. Within Scheme II this can be rationalized by assuming that the equilibrium constant  $K_4 = k_4/k_{-4}$  is shifted toward the neutral tetrahedral intermediate. This comes as no surprise since the relationship  $\log K_4 - \log K_5 = pK_A(5) - pK_A(HN_3) \geq 5$  is expected to hold.<sup>37</sup> When  $N_3^-$  is used as nucleophile, the presence of any proton donor should increase the rate. Indeed, the observed rate increased linearly with the concentration of added  $H_2PO_4^-$  resulting in a sixfold enhancement at  $1 \text{ M } H_2PO_4^-$ . By use of eq 1 and a reasonable  $k_{-6}$  for  $H_2PO_4^- \approx 10^8 \text{ M}^{-1} \text{ s}^{-1}$   $k_8 \approx 2 \times 10^7$  could be estimated. Although several assumptions are involved, an agreement with the value of the upper limit of  $k_x$  as determined from eq 2 is found. While the assumption of  $(\Delta S)_x^* \approx 0$  for  $k_8$  seems reasonable, protonation by water is expected to entail a negative activation entropy. Thus, the above agreement indicates that  $k_{-6}(H_2O) < k_8 \approx 10^7$ . The upper limit of  $k_{-6}(H_2O)$  in combination with the assumption of a diffusion controlled rate constant (i.e.,  $10^9\text{--}10^{10} \text{ M}^{-1} \text{ s}^{-1}$ )<sup>24</sup> for the deprotonation of **5f** (with  $Nu^-$  being  $N_3^-$ ) by  $OH^-$  implies that  $pK_A(5f) < 12$ .<sup>37</sup>

(23) Merenyi, G.; Lind, J. *The Fifth Tihany Symposium on Radiation Chemistry*; Akademiai Kiado: Budapest, 1983; p 103.

(24) Eigen, M. *Angew. Chem., Int. Ed. Engl.* 1964, 3, 1.



In the addition of H<sub>2</sub>O to the diazaquinones **2** both the measured activation parameters and the solvent kinetic isotope effect are strikingly similar to the values found for the neutral hydrolysis of certain esters.<sup>25-27</sup> Therefore, the transition state is proposed to involve two water molecules as has been suggested in the literature for ester hydrolysis.

The substituted anilines are an interesting class of nucleophiles revealing much about the manner in which the transition state is formed. The presence of a pronounced general base catalysis, similar to that found in the aminolysis of esters,<sup>28</sup> is consistent with nucleophilic addition. Clearly, water also acts as a general base abstracting a proton from the amino nitrogen in the transition state. The very low activation enthalpies measured probably derive from the latter process. Since the  $\Delta H^\ddagger$  values are low and similar for all the investigated anilines, the large span in the rate constants (five orders of magnitude) is completely governed by the entropies of activation. As can be seen from Table IV the observed rates also show a monotonic dependence on the p*K*<sub>a</sub>'s of the conjugate acids. Thus, the size of the nitrogen lone pair emerges as the decisive factor in determining the rate constant. The larger the latter the looser the transition state will be, thus imposing smaller restrictions on the rotation of the moieties. Hence the more positive activation entropies. This interpretation also explains why the 2,6-substituted anilines do not show the effect of steric crowding.

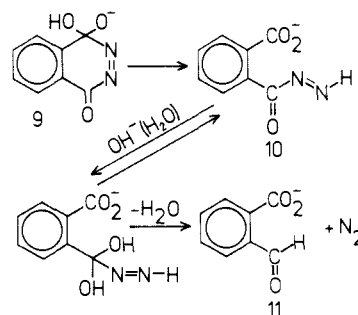
The low p*K*<sub>a</sub>'s of the ortho alkyl substituted anilines as compared to unsubstituted analogues have been ascribed to a diminished solvation of the cations. Allowing for this effect Wepster<sup>29</sup> has estimated the "normal" p*K*<sub>a</sub>'s of 2-methyl- and 2,6-dimethylaniline to be 5.04 and 5.39, respectively. The latter values relate better to the observed rate constants (Table IV). If Wepster's interpretation is correct this would imply that solvation of the quaternary nitrogen plays a minor rôle in the transition state.

Figure 3 reveals that the anilinium cation reacts slower than aniline. However, the reverse is true of the conjugate acid of *o*-bromoaniline and probably also for other substituted anilines with low p*K*<sub>a</sub> values. The nice fit to the p*K*<sub>a</sub> values of the corresponding anilinium cations shows that no specific acid catalysis operates. Now, since nucleophilic addition presupposes the presence of a free lone pair on the aniline nitrogen the reactivity of the conjugate acids can be interpreted in either of two ways. (1) The cation protonates the carbonyl oxygen thereby creating a caged pair of neutral aniline and protonated diazaquinone. Then the cage pair collapses rapidly and irreversibly into a tetrahedral intermediate. (2) Protonation of the carbonyl oxygen and addition of the anilinic nitrogen to the carbonyl carbon occur concertedly via a four-center transition state. The finding that the conjugate acid of some anilines reacts faster than the base with diazaquinones clearly militates against the reaction being an electron transfer. Furthermore, with typical  $\lambda^\circ$  values<sup>6,30</sup> the Marcus equation

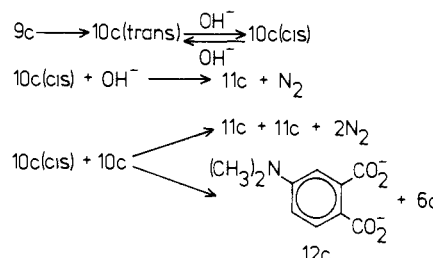
$$\Delta G^\ddagger = \frac{\lambda^\circ}{4} \left( 1 + \frac{\Delta G^\circ}{\lambda^\circ} \right)^2$$

predicts rate constants which are lower by about five orders of magnitude than the measured ones. More specifically, luminol (**3b**) (which can be viewed as an aniline) reacts with **2b** with almost the same rate as aniline itself.<sup>9</sup> Note, however, that the oxidation potential of luminol is more positive by about 300 mV than that of aniline.<sup>31,32</sup> Now, an electron transfer between luminol and **2b** would produce two semiquinone radicals. However, as Scheme I shows, it is precisely the reverse reaction, i.e., dismutation of

Scheme III



Scheme IV



the radicals which provides the whole basis of the present work. The absence of N<sub>2</sub> as a product indicates that the anilinic tetrahedral intermediate **5** does not break down into an acyl diazene species.

**The Hydrolysis.** The conductimetric monitoring of the hydrolyses of **2a** and **2c** at pH 9.8 and 10.7 shows that monoanions are formed with rates which equal the initial addition of OH<sup>-</sup>. The finding that hydrolysis of **2a** and oxidation of **6** yield the same species implicates **10a** as the intermediate monoanion. Obviously, the rate with which the tetrahedral intermediate anion **9a** breaks down into **10a** exceeds 2·10<sup>4</sup> s<sup>-1</sup>, the measured conductivity rate at pH 10.7. By the same token the breakdown rate of **9c** must be higher than 5·10<sup>3</sup> s<sup>-1</sup>.

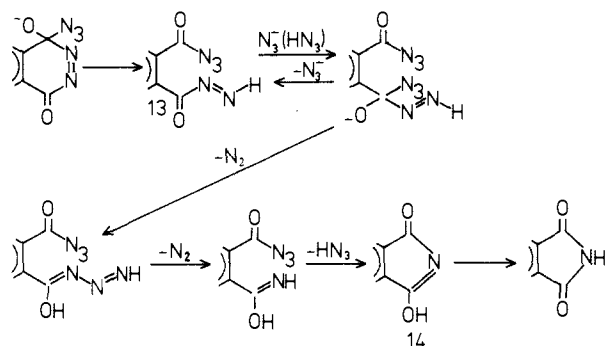
With **2a** as parent the rate-determining step in the formation of the end products is the hydrolysis of **10a** (Scheme III). In analogy with **2a** we expect this reaction to proceed via a tetrahedral intermediate. A measure of the substituent effects is obtained by comparing the rates of the alkaline hydrolyses of **2a** ( $k = 5 \times 10^7$  M<sup>-1</sup> s<sup>-1</sup>), **10a** ( $k = 5.6 \times 10^3$  M<sup>-1</sup> s<sup>-1</sup>), and **8** ( $k = 5 \times 10^3$  M<sup>-1</sup> s<sup>-1</sup>). Clearly, a carbonyl group in ortho position to the reactive center has a dramatic effect.

In contrast to the simple reaction pattern of species **10a** the chemistry of the corresponding species derived from **2c** is complex. The slight red-shift observed in the spectrum above pH 11 upon the OH<sup>-</sup>-catalyzed first-order transformation of **10c** suggests that the process is a trans to cis isomerization<sup>33a</sup> proceeding via the deprotonated diazene (Scheme IV). If so, this implies that the cis form is thermodynamically more stable than the trans form. As such a process is not observed in the hydrolysis of **2a** it is reasonable to assume that strongly electron-donating substituents can bring about a reversal in stability.<sup>33b</sup> More important for the general mechanism, the above interpretation demands the acyl diazene group to form in the trans configuration. This is only possible if protonation of the N=N<sup>-</sup> group is concerted with the rupture of the tetrahedral intermediate along the C-N bond. Deprotonation of the diazene is then the rate-determining step in the isomerization. Huang et al.<sup>34</sup> have estimated the p*K*<sub>a</sub> of phenyldiazene to be about 19 and showed that the rate of its deprotonation against OH<sup>-</sup> is about 10 M<sup>-1</sup> s<sup>-1</sup>. By comparing

(25) Johnson, S. *Adv. Phys. Org. Chem.* **1965**, *5*, 237-320.  
 (26) Engberts, J. B. F. N. *Water*; Franks, F., Ed.; Plenum Press: New York, 1979; Vol. 6, pp 139-237.  
 (27) Venkatasubban, K. S.; Davies, K. R.; Hogg, J. L. *J. Am. Chem. Soc.* **1978**, *100*, 6125.  
 (28) Challis, B. C.; Butler, A. R. *The Chemistry of the Amino Group*, Patai, S., Ed.; Interscience: London, 1968; pp 280-283.  
 (29) Wepster, B. M. *Recl. Trav. Chim.* **1957**, *76*, 357.  
 (30) Ebersson, L. *Adv. Phys. Org. Chem.*; Gold, V., Bethell, D., Eds.; Academic Press: London, 1982; Vol. 18, pp 116-120.  
 (31) Bacon, J.; Adams, R. N. *J. Am. Chem. Soc.* **1968**, *90*, 6596.  
 (32) Epstein, B.; Kuwana, T. *Photochem. Photobiol.* **1965**, *4*, 1157.

(33) (a) It is a well-known fact that the long wavelength absorption of azo compounds is somewhat stronger for the cis form as compared to the trans form, see: e.g., Inscoc, M. N.; Gould, J. H.; Brode, W. R. *J. Am. Chem. Soc.* **1959**, *81*, 5636. (b) Quantum chemical calculations indicate a relative stabilization of the cis form when H is replaced by CH<sub>3</sub> in HN=NH. See: Merenyi, G.; Wettermark, G.; Roos, B. *Chem. Phys.* **1973**, *1*, 340.  
 (34) Huang, P. C.; Kosower, E. M. *J. Am. Chem. Soc.* **1968**, *90*, 2367.

Scheme V



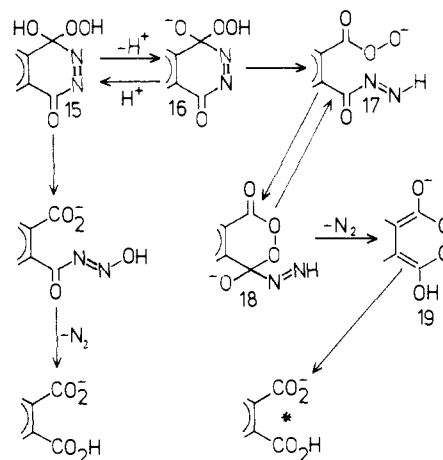
either the  $pK_a$  values of hydroperoxides with peracids or the  $pK_b$ 's of hydrazines with hydrazides we estimate the  $pK_a$  of the acyldiazene to be lower than that of phenyldiazene by about 4  $pK_a$  units, i.e., about 15. The increase in the deprotonation rate from  $10$  to  $5 \times 10^3 \text{ M}^{-1} \text{ s}^{-1}$  is in keeping with the estimated relative acidities.

In contrast to **10a** hydrolysis of the carbonyl in **10c** is only seen at very high  $\text{OH}^-$  concentrations (after trans to cis isomerization). The ratio between the hydrolysis rates ( $\sim 100$ ) reflects the effect of the dimethylamino group. The fact that no second-order reaction is observed below pH 11 merely shows that the trans to cis isomerization is the rate-determining step and has to precede the bimolecular reaction which apparently occurs very slowly in the trans configuration. The participation of diazene species in bimolecular reactions is documented in the literature.<sup>35</sup> The novel feature in the present work is the detection of an  $\text{OH}^-$ -catalyzed isomerization preceding the bimolecular reaction.

While **2a** hydrolyses to yield almost exclusively the formyl benzoate, the end products in the hydrolysis of **2c** are 4-(dimethylamino)formyl benzoate, 4-(dimethylamino) phthalate, and 4-(dimethylamino)phthalic hydrazide in roughly equal amounts.<sup>8</sup> While the formyl benzoate seems to form both in the direct hydrolysis of the acyldiazene and its bimolecular decomposition the formation of the last two products can only proceed via bimolecular dismutation.

**The Azidolysis.** On the basis of the results on the reaction of  $\text{N}_3^-$  with **2a** and **2c** Scheme V appears reasonable. The spectral resemblance between hydrolyzed and azidolyzed **2c** (Figure 6) strongly supports the presence of a  $\text{CO}-\text{N}=\text{NH}$  moiety in both instances. The marked increase in the rate of attack on the acyldiazene moiety upon protonating  $\text{N}_3^-$  is analogous to the azidolysis of the diazaquinone and has been discussed in that context. By comparing certain rate constants the effect of substituents on the carbonyl can be inferred. In the case of **2c** the two observed rates (with a ratio of  $\sim 5$ ) of  $\text{N}_3^-$  attack should pertain to the isomers having the dimethylamino group in meta or para position to the diazene group with the higher value belonging to the meta isomer. Comparing the rate of  $\text{N}_3^-$  attack on **13a** and *p*-**13c** a ratio of  $\sim 100$  is found which tallies with the ratio found for the attack of  $\text{OH}^-$  on the corresponding species **10a** and **10c**. In conclusion, the rate of nucleophilic addition to the acyl diazene group appears to be lowered a 100-fold when a  $(\text{CH}_3)_2\text{N}$  group replaces H in the para position. The ratio of the rates of alkaline hydrolysis of **2a** and **10a** is  $\sim 10^4$ . In contrast, the ratio found in the azidolysis of **2a** and **13a** is merely  $\sim 10$ . This difference shows the decisive role in activating the electrophilic center by replacing an ortho carboxylic group by an active carbonyl. The two subsequent first-order rearrangements are tentatively assigned to the formation of **14** and its isomerization to phthalimide. The similarity between hydrolysis and azidolysis is that the two carbonyl groups initially present are consecutively attacked by the nucleophile. The additional feature in the azidolysis is the intramolecular ring closure to form the phthalimide. The stoichiometry is thus  $2 + \text{NH}_3 \rightarrow \text{phthalimide} + 2\text{N}_2$ . This

Scheme VI



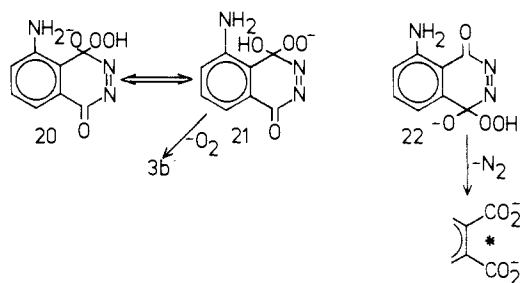
was confirmed by product analysis.

**Chemiluminescence.** The addition of  $\text{H}_2\text{O}_2$  to **2f**, **2b**, and **2c** results in chemiluminescence. Unless we are prepared to consider the perhydrolysis as a curiosity Scheme VI would seem to describe the only reasonable reaction pattern encompassing the entirety of the experimental observations. The ring opening step of the tetrahedral anion **16** is adopted in analogy with the hydrolysis and azidolysis. The peracid anion **17** formed upon the breakdown of **16** should be an excellent intramolecular nucleophile, simple rotation around the  $\text{O}-\text{O}$  bond bringing the terminal oxygen well within bonding distance of the carbonyl carbon. In addition, the peracid group ortho to the diazene carbonyl enhances the electrophilicity of the latter. Then the cyclic tetrahedral intermediate **18** will expel  $\text{N}_2$  rapidly possibly with the aid of  $\text{H}_2\text{O}$ , and the exothermicity of this reaction can be stored in the antiaromatic endoperoxide. The transition from **19** to excited phthalate **12** is invoked from ref 36. In trying to decide which intermediate(s) is (are) responsible for the chemiluminescence dynamics depicted in Figure 12 cognizance should be taken of the following facts and considerations. (1) The pH dependence of the light yield from **2b** in Figure 11 is quantitatively explained by the competition of a pH independent ( $k \sim 1500 \text{ s}^{-1}$ ) and an  $\text{OH}^-$ -catalyzed ( $k_{\text{OH}^-} \approx 10^9 \text{ M}^{-1} \text{ s}^{-1}$ ) breakdown of an intermediate. Therefore, at least up to pH 10 the chemiluminescence rates should pertain to one and the same intermediate. (2) The limiting rate constant at high pH is the same for **2b** and **2c** ( $k \approx 2.5 \times 10^5 \text{ s}^{-1}$ ) while it is slightly lower for **2f** ( $k \approx 1.3 \times 10^5 \text{ s}^{-1}$ ). Thus the process having these rates should be rather insensitive to substituent effects. Also, the activation parameters ( $\Delta H^\ddagger = 44 \text{ kJ/mol}$ ,  $\Delta S^\ddagger = +7 \text{ J/(mol K)}$ ) for both **2b** and **2c**<sup>22</sup> implicate a truly monomolecular process without  $\text{H}_2\text{O}$  assistance. The peracid **17** with a  $pK_a$  of less than 8 would not display the  $\text{OH}^-$  catalysis (see Figure 12) in its ring closure reaction. As will be discussed below the expulsion of  $\text{N}_2$  from **18** is also unlikely to exhibit the  $\text{OH}^-$  catalysis in Figure 12. Finally, the pericyclic reaction leading to the excited phthalate is expected to be independent of the pH in the pertinent interval. Thus, in light of point 1, the  $\alpha$ -hydroxy hydroperoxide **15** emerges as the only reasonable intermediate to account for the chemiluminescent dynamics up to pH  $\sim 10$ . It is safe to assume that the rates of both reactions  $17 \rightarrow 18$  and  $18 \rightarrow 19 + \text{N}_2$  will be diminished by electron-releasing substituents (see the discussion about the azidolysis). Thus, in light of point 2 both **17** and **18** would seem to disqualify. We conclude, therefore, that the species responsible for the chemiluminescence rate at high pH is either **16** or **19**. On the basis of experimental evidence it is not possible to favor either of them.

It follows then that species **15b** has a  $pK_a$ <sup>37</sup> higher or equal to 10.4 and it decomposes with a rate  $\geq 2.5 \times 10^5 \text{ s}^{-1}$ . Figure 11 shows that the light integrals vs. pH of **2b** and **2f** have almost the same  $pK_a$  values. Unless a mere coincidence this finding reveals that the ratio between the neutral and the  $\text{OH}^-$ -catalyzed breakdown rates of  $\alpha$ -hydroxyhydroperoxides **15** is insensitive toward modifications of the aromatic ring. While both the for-

(35) Kosower, E. M. *Acc. Chem. Res.* **1971**, *4*, 193.

Scheme VII



mation and the breakdown of the second tetrahedral intermediate **18** are apparently too rapid to be observable at any pH, their occurrence is strongly implicated in light of our finding in the hydrolysis and azidolysis of diazaquinones.

Some comments about the breakdown of **18** are in order. First, it should be stressed that acyldiazene species are rather stable and expel  $N_2$  only after tetrahedralization of the carbonyl carbon. Now, in the sense of the discussion about the acidity of diazene species the  $pK_a$  of the  $-N=N-H$  group in **18** is estimated to lie between **15** and **19**. Deprotonation of it by  $OH^-$  ions would, therefore, proceed with a rate constant less than  $\sim 10^4 M^{-1} s^{-1}$ . With such a rate being too slow to account for the breakdown of **18** ( $k > 2 \times 10^5 s^{-1}$  at pH 11), we can safely conclude that the process is not  $OH^-$  catalyzed. In our view, the rupture of the C-N bond is concerted with a  $H_2O$ -assisted proton transfer from  $N=N-H$  to the C-O $^-$  group. Obviously, this step proceeds with very low activation energy. Precisely the same considerations should apply to the breakdown of the corresponding tetrahedral intermediates in both hydrolysis and azidolysis.

The pH independent decomposition of **15** yields ground-state phthalate **12**. A simple rupture along the C-N bond would initiate the same reaction sequence as the  $OH^-$ -catalyzed breakdown and thus result in light generation. A concerted rupture of both the C-N bond and the O-O bond of **15** would account for the absence of chemiluminescence. The activation parameters of this reaction ( $\Delta H^\ddagger = 25 \text{ kJ mol}^{-1}$ ,  $\Delta S^\ddagger = -104 \text{ J mol}^{-1} K^{-1}$ ) point to a structured transition state with the probable participation of water molecules. The upper limit for the rate constant of the pH independent chemiluminescent breakdown of **15**, i.e., a simple C-N bond rupture, can be estimated as follows. A plot of  $\int_0^\infty I dt$  vs.  $[OH^-]$  in the pH range 6.3–7.2 is linear with an intercept close to 0. Allowing for the errors in the slope, the intercept, and the measured rate of  $OH^-$  catalysis we find  $0 < k_{15 \rightarrow 17} < 5 s^{-1}$ .

In the case of **2b** the increase in phthalate yield with decreasing pH is consistent with a partial production of the hydrazide and  $O_2$  from **16b** but none from **15b**. Our view that the cyclic hydrazide and  $O_2$  is unlikely to form after the rupture of **16b** along

the C-N bond is supported by the finding that in basic media the open hydrazide **6** does not isomerize to its cyclic analogue. Now, since the initial addition of  $HO_2^-$  to **2b** proceeds without a barrier (see Table III) **20** and **22** (see Scheme VII) are expected to form in essentially equal amounts. The fact that both **2a** and **2f** yield the phthalate quantitatively reveals that hydrazide formation is connected with the amino group in a ortho (or para) position with respect to the tetrahedral carbon. Therefore, a natural way to account for the ca. 50% yield of the hydrazide from **16** is to assume that **20** yields mostly the hydrazide with very little phthalate while the reverse is true of **22**. A plausible rationale for this view is that species **20** may tautomerize to **21** from which facile expulsion of  $O_2$  according to Scheme VII is expected. From the above considerations **22** would emerge as the major chemiluminescing species. Similar arguments apply to both **2c** and **2d**.

#### Unifying Features in Hydrolysis, Azidolysis, and Perhydrolysis.

All three systems studied in this work implicate the formation of a tetrahedral intermediate which subsequently breaks down by the expulsion of molecular nitrogen. In the hydrolysis and azidolysis the formation of the intermediate is seen kinetically and occurs through the addition of  $OH^-$  or  $N_3^-$  to the acyldiazene species. In the perhydrolysis, this process is intramolecular and too rapid to be observed.  $N_2$  expulsion is an exothermic process, and the energy can be utilized in different ways. In the hydrolysis the process probably results in the formation of a carboanion which protonates to yield the aldehyde hydrate whence the aldehyde is obtained through dehydration. In the azide adduct, the liberated energy is pooled into the azide moiety and brings about a rupture into  $N_2$  and a nitrene group. This is the thermal equivalent of the photochemical decomposition of azide. Finally, in the perhydrolysis the energy of  $N_2$  expulsion from **18** is utilized in the generation of an antiaromatic endoperoxide with similar energy content and orbital symmetry as the excited phthalate. Therefore, this species is ideally suited for the chemiexcitation process.<sup>36</sup>

**Acknowledgment.** We are greatly indebted to the staff of the Dept. of Organic Chemistry. The contributions of Drs. P. Sand and J. Siden in synthetic work have been especially valuable. We are also grateful to S. Samuelsson for his technical assistance. The Swedish Natural Science Research Council is acknowledged for financial support.

**Registry No.** **2a**, 20116-64-7; **2b**, 60851-83-4; **2c**, 71982-97-3; **2f**, 21389-20-8; **3a**, 1445-69-8; **3b**, 521-31-3; **3c**, 18697-31-9; **3f**, 21389-21-9.

(36) Ljunggren, S.; Merenyi, G.; Lind, J. *J. Am. Chem. Soc.* **1983**, *105*, 7662.

(37) Tee, Trani, McClelland, and Seaman (Tee, O. S.; Trani, M.; McClelland, R. A.; Seaman, N. E. *J. Am. Chem. Soc.* **1982**, *104*, 7219) have reported that the pseudobase of the 4-oxoquinazolinium cation has a  $pK_a$  of 11.1. This compound is somewhat similar to **5** so we expect the  $pK_a$  of the latter to be  $11 \pm 1$ .